

# Intelligent Reflecting Surfaces (IRS) Metasurface-based with Tunable Varactor Diodes for Advanced 6G Wireless Applications

Hadumanro Malau  
*Department of EEE*  
*University College London*  
London, United Kingdom  
hadumanro.malau.19@ucl.ac.uk

Kin-Fai Tong  
*Department of EEE*  
*University College London*  
London, United Kingdom  
k.tong@ucl.ac.uk

Kai-Kit Wong  
*Department of EEE*  
*University College London*  
London, United Kingdom  
kai-kit.wong@ucl.ac.uk

**Abstract**—Intelligent Reflecting Surfaces (IRSs) stand as pivotal technology for augmenting the efficiency and performance of 5G wireless networks. However, the deployment of these surfaces, especially in the Ka-band (26 GHz and beyond) for the prospective 6G networks, encounters challenges regarding bandwidth limitations and restricted reflection phase ranges in their unit cells. Addressing these issues is crucial to harnessing the full potential of IRS metasurface-based unit cells.

This paper presents a design scenario for IRS metasurface-based unit cells, leveraging varactor diodes to enable real-time reconfiguration. The dynamic modification of the metasurface's fundamental structure allows for adaptive alterations in its electromagnetic properties, pivotal in addressing challenges such as bandwidth constraints and limited reflection phase range crucial for future wireless applications. By employing varactor diodes, this research study achieves a dynamic tuning capability within the IRS metasurface-based unit cell, facilitating extensive beam steering across a broad reflection phase range of  $343^\circ$  within the Ka-Band spectrum. The integration of these diodes enables real-time control over the radiation field at the unit cell's surface, elevating parameters such as signal-to-noise ratio (SNR), efficiency, and gain, pivotal for optimal wireless communication.

The simulation outcomes emphasize the superiority of the proposed Intelligent Reflecting Surface (IRS) design over traditional passive reflectors, showcasing its potential to significantly enhance the performance of forthcoming 6G wireless networks. This research paves the way for controllable IRS metasurface arrays with beam steering functions, poised to revolutionize Ka-Band and mm-Wave applications, overcoming current limitations and unlocking unprecedented capabilities for future wireless networks.

**Keywords**—intelligent reflecting surfaces, metasurface, tunable varactor diodes, Ka-band

## I. INTRODUCTION

Mobile data traffic has seen continual growth over the past decade, and by the year 2021, the global data traffic is expected to have grown 23 times compared to the amount of traffic on the entire Internet in 2005. The International

Telecommunication Union (ITU) report forecasts an incredible surge in global mobile data traffic, estimating a staggering five zettabytes (ZB) per month by 2030. This increase will coincide with data rates expected to soar to 1 Tb/s [1]. As well as being able to support extremely high data rates, there are several other heterogeneous services expected to be offered by future wireless networks, such as localization, low-latency, and ultra-reliable communication systems.

It is evident that expanding the bandwidth emerges as a viable approach to accommodate the substantial surge in data volume. As per preliminary discussions, frequencies ranging from 26 GHz and higher are under consideration for 6G technology. These bands offer ample spectrum availability to meet the anticipated requirements [2]. Nevertheless, current wireless communication faces several challenges that will demand substantial efforts for resolution. Some of these concerns are already being discussed and addressed in the 5G standard, such as susceptibility to obstruction, sampling, and the functionality of A/D and D/A circuits for signal conversion, along with considerations regarding their communication range. Additionally, when operating at higher frequencies, the significant challenges encompass the miniaturization and assembly of antenna models alongside their associated circuitry. This effort must concurrently enhance various antenna properties, including bandwidth, operating frequency range, and reflection phase shifting range, while also addressing issues such as noise suppression and mitigating inter-component interference. These hurdles represent pivotal areas demanding comprehensive solutions.

An IRS array consisting of metasurface-based elements are extremely thin, generally exhibiting a thickness significantly smaller than the electromagnetic wavelength. It possesses distinctive properties absent in natural materials, offering unique electromagnetic characteristics [3]. The distinctive characteristic of this IRS metasurface-based array lies in

its capacity to customize electromagnetic waves in diverse manners. Consequently, employing these technologies could enhance the reliability of data transfer and processing. They also form an ideal distribution platform for low-power and low-complexity sensors, capacity, and analog computation. The convergence of these distinctive attributes—comprising high controllability of radio waves, scalability in deployment, and the accompanying economic advantages—positions IRS metasurfaces as a pivotal technology capable of supporting forthcoming wireless networks, despite the intricate demands they present.

Incorporating controllable electronic components into unit cells within an IRS-metasurface design enables tunability and reconfigurability. To accomplish this objective, diverse conventional tuning methods are employed, including diode, liquid crystal, and piezoelectric mechanisms, along with the utilization of varactor diodes [4]. This paper utilizes varactor diodes. It presents several benefits, including high-frequency operation, a substantial tuning ratio for capacitance, and minimal power consumption. Through the application of a biasing voltage, the varactor diode within an Intelligent Reflecting Surface (IRS) can undergo tuning. The capacitance of a varactor diode shows an inverse relationship with the applied bias voltage. In the IRS setup, modulating the biasing voltage allows control over the varactor diode’s capacitance, consequently influencing the reflective properties of the unit cell. Hence, the manipulation of the bias voltage applied to the varactor diode within each unit cell enables dynamic control over both the amplitude and direction of the reflected signal.

In the realm of research literature, particularly concerning Ka-Band or 6G applications, there remains a scarcity of studies involving IRS metasurface-based configurations characterized by substantially smaller sizes and spacings compared to the wavelength, typically ranging from 1/4 to 1/10 of the wavelength. An investigation conducted by Wankai and his colleagues examined the potential of using IRS metasurface-based with varactor diodes in the lower operating spectrum of 4 GHz [5]. Two commercial varactor diodes, specifically the SMV2019-079LF models manufactured by Skyworks Solutions, Inc., exhibit a capacitance range between 2.31 and 0.24 pF when reverse voltage bias is applied in the middle of two metal strips positioned between them.

The experimental results demonstrate a 500 MHz bandwidth at 3.5-4 GHz operating frequency and a reflected phase shift range of 255° at 4 GHz in phase under different biasing voltages. Another paper [6] explored the potential of incorporating the MA46H120-ODS1203 varactor diode from MACOM in a K-shaped unit cell design for Ku-Band applications, showcasing a capacitance range of 0.14 pF to 1.14 pF. It offers a 1.3 GHz bandwidth with a phase dynamic range exceeding 270° spanning from 11.5 GHz to 12.8 GHz. While the outcomes exhibit promise, they are not yet deemed

adequate for Ka-Band applications.

Hence, this paper is driven by the objective of devising a novel unit cell based on IRS metasurfaces utilizing varactor diodes. The aim is to achieve a bandwidth of up to 2 GHz and a phase dynamic range exceeding 270°, features that align with the requisites for upcoming 6G network applications. Section 2 of this paper will outline the basic design of the proposed unit cell within the IRS metasurface, employing varactor diodes, specifically the SMV2019-079LF models by Skyworks Solutions, Inc. In Section 3, we analyze and demonstrate the results. Section 4 will culminate by summarizing the benefits and potential applications of employing adjustable IRS metasurface-based unit cells.

## II. THE THEORY AND BASIC IRS UNIT CELL DESIGN

The proposed IRS metasurface-based unit cell is a square geometry unit cell with the width of the substrate  $W = 7$  mm and the length of the metal strip  $L = 5.628$  mm, printed on a grounded dielectric substrate of 0.7875 mm in height with  $\epsilon_r = 2$  and  $\tan \alpha = 0.0021$ . There are four splits along the center of the L-shaped metal strips, each characterized by a specific gap size ( $d$ ).

The magnetic resonance is determined by the metal strip width ( $s$ ) and the gap width ( $d$ ) [7]. The surface consists of two L-shape metal strips on the left side and an I-shape metal strip on the right side of the metasurface unit cell. The magnetic resonance is determined by the metal strip width ( $s$ ) and the gap width ( $d$ ), as shown in Fig. 1.

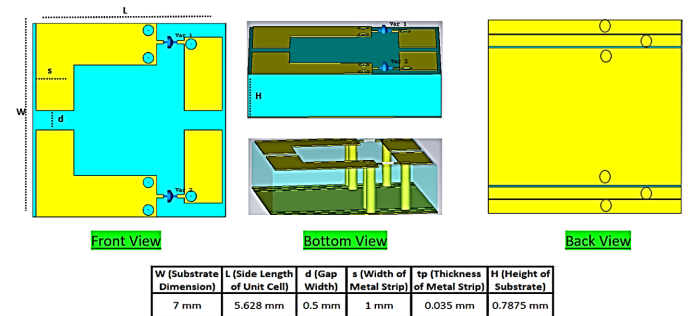


Fig. 1. Proposed IRS unit cell design with two varactor diodes

An equivalent lumped circuit is shown in Fig. 2 below to model the proposed unit cell [8]. The calculation of the dynamic capacitance range for the unit cell is computed by considering its equivalent circuit as follows:

$$\begin{aligned}
 C_{min} + C_{total} < C < +C_{total} + C_{max} \\
 C_{min} + C_{gap/4} < C < +C_{gap/4} + C_{max} \\
 C_{min} + C_{sp} + C_{pp} < C < +C_{sp} + C_{pp} + C_{max} \quad (1)
 \end{aligned}$$

Where:

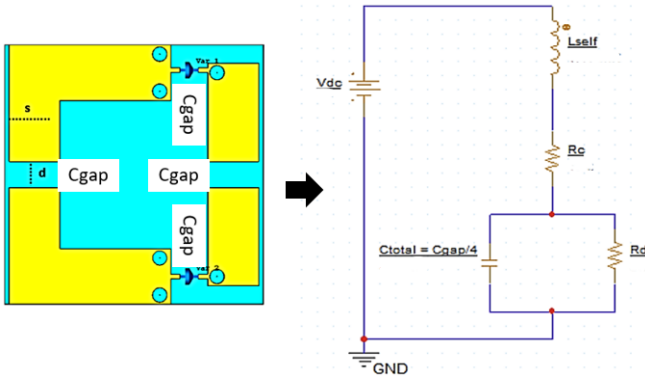


Fig. 2. The equivalent lumped circuit of proposed metasurface unit cell design

- $C_{sp}$  = Capacitance value of serial gaps of the metal ring
- $C_{pp}$  = Capacitance value of parallel gaps of the metal ring
- $C_{gap}$  = Equivalent gap capacitance
- $L_{self}$  = Total self-inductance of the metal ring

The total conductor losses ( $R_c$ ), which are indicated by the resistance, can be computed using the following equation:

$$R_c = \frac{4L}{\sigma \delta 2(s + tp)} \quad (2)$$

with:

$$\delta = \frac{1}{\sqrt{\pi f_c \mu \sigma}} \quad \text{and} \quad \sigma = \omega \epsilon \tan \alpha$$

The resistance representing dielectric losses ( $R_d$ ) surrounding the gaps can be acquired through the following formula:

$$R_d = \frac{d}{(\tan \alpha) (\omega \epsilon) sH} \quad (3)$$

where:

- $L$  = Length of the unit cell
- $\sigma$  = conductivity of the metal =  $5.96e^7$  S/m
- $\delta$  = skin depth of the metal ring
- $tp$  = thickness of the metal
- $H$  = thickness of the substrate
- $\omega$  = angular frequency =  $2 \pi f_c$ , e.g.  $f_c = 26$  GHz
- $\tan \alpha$  = loss tangent of the substrate = 0.0021

The impedance  $Z$  for the circuit model of the proposed unit cell above can be derived as follows:

$$Z = R + jX \quad (4)$$

$$Z = \left( R_c + \frac{R_d}{1 + \omega^2 C^2 R_d^2} \right) + j \left( \omega(L_{self}) - \frac{\omega R_d^2 C}{1 + \omega^2 C^2 R_d^2} \right)$$

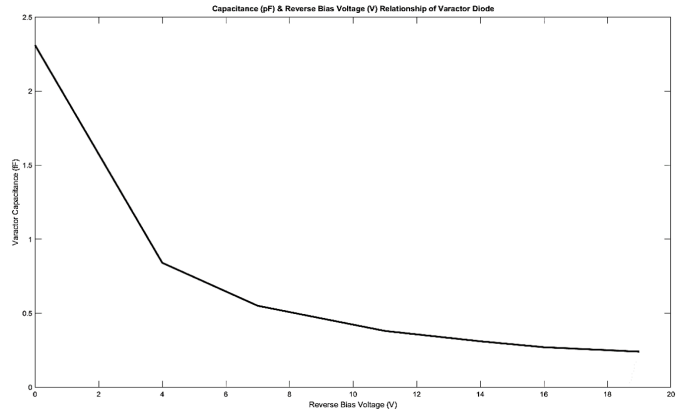


Fig. 3. Reverse voltage bias of different capacitance of varactor diode

The reflection coefficient ( $\Gamma$ ) of above proposed unit cell is derived from its total equivalent load impedance  $Z$  (a unit cell) and the impedance towards the source at free-space  $Z_0$  ( $377 \Omega$ ), can be written as [9]:

$$\Gamma = \frac{(Z_{aunitcell}) - Z_0}{(Z_{aunitcell}) + Z_0} \quad (5)$$

$$\Gamma = \frac{(R_c + \frac{R_d}{1 + \omega^2 C^2 R_d^2}) + j\omega(L_{self}) - \frac{R_d^2 C}{1 + \omega^2 C^2 R_d^2} - Z_0}{(R_c + \frac{R_d}{1 + \omega^2 C^2 R_d^2}) + j\omega(L_{self}) - \frac{R_d^2 C}{1 + \omega^2 C^2 R_d^2} + Z_0}$$

Finally, the reflection phase of the equivalent circuit ( $\varphi$ ) of the proposed IRS unit cell above can be defined as:

$$\varphi = \arctan \left( \frac{\text{Im} \frac{Z - Z_0}{Z + Z_0}}{\text{Re} \frac{Z - Z_0}{Z + Z_0}} \right) \quad (6)$$

$$\varphi = \arctan \left( \frac{j\omega(L_{self}) - \frac{R_d^2 C}{1 + \omega^2 C^2 R_d^2} - Z_0}{j\omega(L_{self}) - \frac{R_d^2 C}{1 + \omega^2 C^2 R_d^2} + Z_0} \cdot \frac{(R_c + \frac{R_d}{1 + \omega^2 C^2 R_d^2}) - Z_0}{(R_c + \frac{R_d}{1 + \omega^2 C^2 R_d^2}) + Z_0} \right)$$

Two commercially available varactor diodes, the SMV2019-079LF models by Skyworks Solutions, Inc., with capacitance varies from 0.24fF to 2.31fF when reverse voltage bias are applied varies in the range between 0V and 20V in the gaps which connect the two L-shaped metal strips with the I-metal strip. Fig. 3 above illustrates the correlation between the applied voltage and the junction capacitance of a varactor diode.

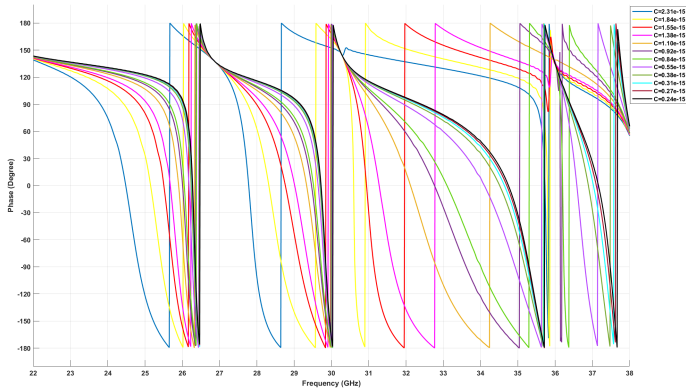


Fig. 4. Reflection phase as a function of frequency for different values of capacitance of two varactor diodes

### III. RESULTS AND DISCUSSION

The reflection of the IRS metasurface-based unit cell was simulated using the TEM floquet port in Microwave CST Studio [10]. An investigation was conducted utilizing reflection simulations on a unit cell under normal incidence. Sweep capacitance values with  $C_{max} = 2.31$  fF,  $C_{min} = 0.24$  fF, of two varactor diodes, Var1 and Var2, underwent reverse bias voltages of 0V and 20V to observe their impact on the metasurface unit cell parameters. It's crucial to highlight that the physical integration of these two varactor diodes within the metal patch subjects our unit cell to parasitic gap capacitance. Given the minimal dielectric capacitance in this specific unit cell implementation, this aspect requires careful consideration [11].

Fig 4 illustrates the reflection phase (in degrees), while Fig. 5 displays the magnitude of the reflection coefficient (in dB) concerning frequency across various capacitance values of the two varactor diodes. The graph in Fig. 5 indicates the operational frequency range suitable for the Ka-Band, where the magnitude of reflected (dB) is more than -3 dB are available at 26 - 30 GHz, 31.5 - 35 GHz, and 36.5 - 38 GHz, respectively.

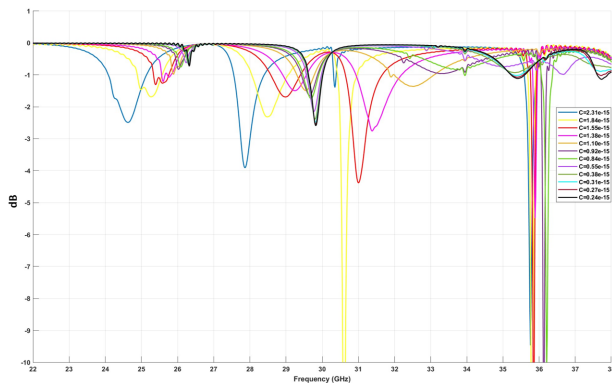


Fig. 5. The magnitude of the reflection coefficient varies with frequency across different capacitance values of two varactor diodes

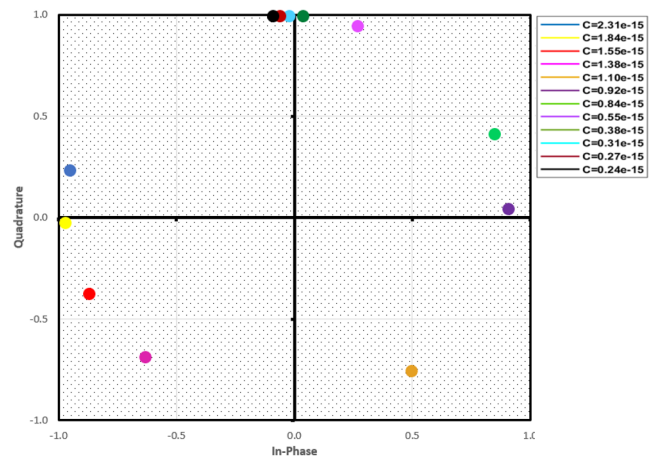


Fig. 6. Variations in the in-phase and quadrature components of the reflection coefficient at 26 GHz in response to alterations in biasing voltage

Moreover, through an examination of the biasing voltage and frequency, it becomes feasible to ascertain the phase of the reflection coefficient. Utilizing this data allows for the management and optimization of IRS surfaces concerning their reflective properties. A control of the phase properties of the reflection coefficient will enable the reflected wave to be guided in a specific direction, thereby improving the signal-to-noise ratio (SNR), and increasing the capacity of 6G networks.

Above, the prospective operating frequency bands for future 6G wireless applications, specifically the Ka-band, are noted at 26 GHz and 31.5 GHz. Simulation results demonstrate that the reflection phase ranges from  $289^\circ$  to  $325^\circ$  at these frequencies. Fig. 6 and Fig. 7 illustrate the in-phase and quadrature components of the reflection coefficient at both operating frequencies, respectively.

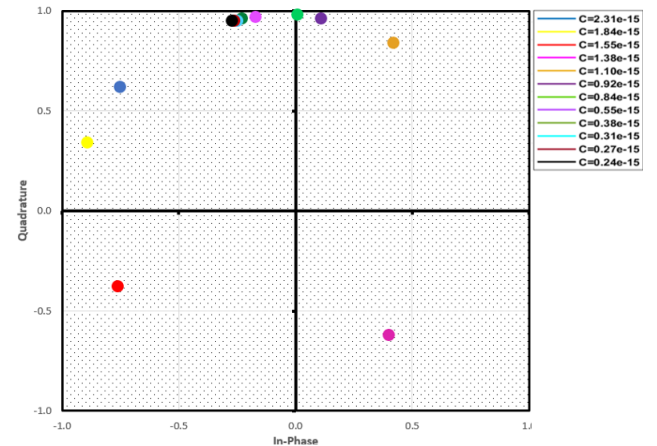


Fig. 7. Variations in the in-phase and quadrature components of the reflection coefficient at 31.5 GHz in response to alterations in biasing voltage

The graph in Fig. 8 below shows the maximum reflection phase range (in degrees) of an IRS metasurface-base unit cell at different operating frequencies in Ka-Band (in GHz).

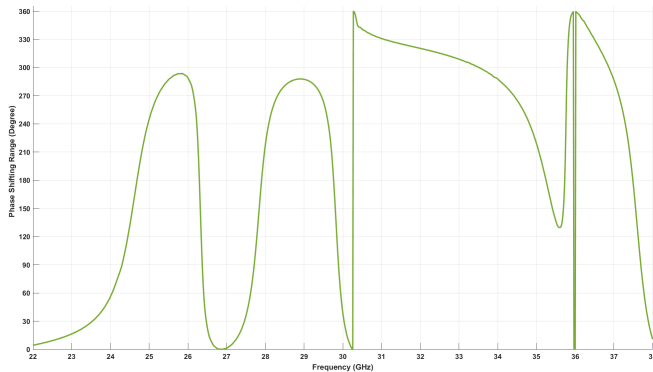


Fig. 8. The reflection phase range exhibited by the proposed IRS unit cell

The maximum reflection phase range varies significantly with different frequencies. At 36.3 GHz, the peak reflection phase range reaches  $343^\circ$ , displaying the highest value, while the minimum reflection phase range of  $217^\circ$  is noted at 28 GHz. At frequencies of 26, 29, 31.5, 32, 33, and 34 GHz, the peak reflection phase ranges from  $287^\circ$  to  $325^\circ$ .

The specifics of the maximum reflection phase range at various operating frequencies are presented in Table 1. The ability of the IRS unit cell to manipulate the reflection phase across a broad spectrum of frequencies proves advantageous, since it allows it to adjust the direction of reflected electromagnetic waves and steer them in various directions. An IRS unit cell with a wider reflection phase range enables the steering of reflected beams over a broader range of angles.

TABLE I  
THE REFLECTION PHASE RANGE BY THE PROPOSED IRS UNIT CELL

Operating Frequency (GHz)	Maximum Reflection Phase Range ( $^\circ$ )
26	289
28	217
29	287
30	39
5	45
31.5	325
32	320
33	308
34	287
35	219
36.3	343
37	286

Therefore, the beam scanning process can encompass a broader spectrum of angles. Similarly, when the reflection phase range of an IRS unit cell is narrower, it confines the

scope of angles available for beam scanning. Consequently, the IRS lacks the capacity to manipulate the reflection phases of the unit cells to direct reflected beams toward specific directions.

#### IV. CONCLUSION

In the pursuit of advancing IRS metasurface-based unit cells for optimal performance, particularly in the realm of Ka-Band and 6G network applications, this study has uncovered critical challenges. The limitations posed by the narrow bandwidth and restricted reflection phase range within these cells remain substantial barriers to their full potential. To confront these hurdles, this report has presented and thoroughly examined a design scenario focused on IRS metasurface-based unit cells.

The core of this paper lies in the utilization of varactor diodes within IRS metasurface-based unit cells, enabling real-time reconfiguration. This dynamic adaptability alters the fundamental structure of the metasurface, thereby modifying its electromagnetic characteristics. The pursuit of dynamic tunability becomes paramount in wireless applications to enhance critical unit cell parameters like bandwidth, signal-to-noise ratio (SNR), efficiency, and gain.

Through this exploration, an IRS metasurface-based unit cell capable of steering beams across an extensive reflection phase range of  $343^\circ$  has been introduced. Operational within the Ka-Band spectrum, this unit cell, empowered by two varactor diodes, grants dynamic control over the radiation field at its surface. This design not only holds promise for inclusion within larger-scale IRS arrays but also signifies a leap in steering capabilities. It underscores the potential of controllable IRS metasurface arrays with beam steering functions for upcoming Ka-Band and mm-Wave applications.

However, to fully realize the effectiveness of this proposed methodology, it's imperative to address ongoing obstacles, such as optimizing the diode's efficiency and mitigating non-linear effects, while also exploring scalability within larger metasurface arrays. Overcoming these challenges will pave the way for a more robust and impactful implementation of IRS metasurface-based units in future wireless communication systems.

#### REFERENCES

- [1] Report ITU-R M.2370-0, IMT traffic estimates for 2020 to 2030, Geneva: Electronic Publication, 2015.
- [2] European Commission: Directorate General for Communications Networks, Content, and Technology, The development of 6G and possible implications for spectrum needs and guidance on the rollout of future wireless broadband networks, Brussels: Radio Spectrum Policy Group, 14 June 2023.
- [3] E. Basar, et al., "Wireless communications through reconfigurable intelligent surfaces," *IEEE Access*, vol. 7, August 2019.

- [4] Francesca Venneri, Luigi Boccia, et al., "Analysis and design of passive and active microstrip reflectarrays," Wiley Periodicals, Inc. Int J RF and Microwave CAE 13: 370–377, 2003.
- [5] Jun Yan Dai, Wan Kai Tang, et al., "Wireless communications through a simplified architecture based on time-domain digital coding metasurface," Adv. Mater. Technol, 2019.
- [6] Jing Nie, Yan-Qing Tan, et al., "Analysis of Ku-band steerable metamaterials reflectarray with tunable varactor diodes," Progress in Electromagnetic Research Symposium (PIERS), 2016.
- [7] D. M. Pozar, S. D. Targonski, and H. D. Syrigos, "Design of millimeter-wave microstrip reflectarrays," IEEE Transactions on Antennas and Propagation, vol. 45, no. 2, pp. 287–296, 1997.
- [8] Constantine A. Balanis, "Antenna Theory Analysis and Design," New York: John Wiley and Sons, 2<sup>nd</sup> Edition, 1997.
- [9] P. Nayeri, F. Yang, and A.Z. Elsherbeni, "Reflectarray Antennas: Theory, Designs, and Applications," New York: John Wiley and Sons, 2018.
- [10] Francesca Venneri, Luigi Boccia, et al., "Analysis and Design of Passive and Active Microstrip Reflectarrays," Wiley Periodicals, Inc. Int J RF and Microwave CAE 13: 370–377, 2003.
- [11] W. Tang, et al., "Wireless communications with programmable metasurface: New paradigms, opportunities, and challenges on transceiver design," IEEE Wireless Communications, 2019.